is grateful to The Danish Ministry of Energy. B.K., H.G., and C.B. gratefully acknowledge generous support by the Fonds der Chemischen Industrie.

Supplementary Material Available: Tables SIV and SV, listing anisotropic temperature factors and L and T tensors from the librational analysis of $AlCl_4^-$ (2 pages); Tables SI-SIII, listing observed and calculated structure factors of $NaAlCl_4$ at three different temperatures, 138, 150, and 154 °C, respectively (13 pages). Ordering information is given on any current masthead page.

Contribution from the Department of Chemistry, University of Minnesota, Minneapolis, Minnesota 55455

Heterobimetallic Au-Pd Cluster Complexes. X-ray Crystal and Molecular Structures of $[(CO)Pd(AuPPh_3)_8](NO_3)_2$ and $[(P(OCH_3)_3)Pd(AuPPh_3)_6(AuP(OCH_3)_3)_2](NO_3)_2$

Larry N. Ito, Anna Maria P. Felicissimo,† and Louis H. Pignolet*

Received August 24, 1990

In this paper we report the nucleophilic addition/substitution reactions of tertiary phosphites $P(OMe)_3$ and $P(OCH_2)_3CCH_3$ to the 16-electron clusters $[Pd(AuPPh_3)_8]^{2+}$ (**1**) and $[(PPh_3)Pd(AuPPh_3)_6]^{2+}$ (**3**) to give the new 18-electron compounds $[(P(OCH_3)_3Pd(AuPPh_3)_6(AuP(OCH_3)_3)_2]^{2+}$ (**5**) and $[(P(OCH_2)_3CCH_3)_2Pd(AuPPh_3)_6]^{2+}$ (**4**), respectively. These compounds have been characterized by IR spectroscopy, FABMS, and ^{31}P and ^1H NMR spectroscopy. An electrochemical study of **1** has also been carried out. The 16-electron cluster undergoes two reversible single-electron reductions to the neutral 18-electron compound $[Pd(AuPPh_3)_8]^0$. The reaction of **1** and **3** with CO has also been investigated with the result that only **1** gives a product, $[(CO)Pd(AuPPh_3)_8](NO_3)_2$ (**2**). X-ray crystal structure determinations have been carried out on the 18-electron clusters **2** and **5**, and their metal core geometries, which are spheroidal fragments of centered icosahedrons, are in agreement with predictions based on electron counting. The crystal data for these compounds are as follows: for **2**, triclinic $P\bar{1}$, a = 16.23 (1) Å, b = 16.94 (2) Å, c = 30.78 (1) Å, α = 89.63 (6)°, β = 87.61 (5)°, γ = 62.54 (7)°, V = 7496 Å^3, Z = 2, residuals R = 0.075 and R_w = 0.085 for 9559 observed reflections and 718 variables, Mo Kα radiation; for **5**, triclinic $P\bar{1}$, a = 18.577 (3) Å, b = 19.248 (3) Å, c = 21.963 (8) Å, α = 82.00 (2)°, β = 78.16 (2)°, γ = 74.90 (2)°, V = 7390 Å^3, Z = 2, residuals R = 0.060 and R_w = 0.069 for 4465 observed reflections and 346 variables, Mo Kα radiation.

Introduction

Recently, we reported the synthesis and characterization of the first metal cluster compounds that contain Pd-Au bonds.[1] The $NaBH_4$ reduction of a CH_2Cl_2 solution that contains $Pd(PPh_3)_4$ and $Au(PPh_3)NO_3$ led to the formation of $[Pd(AuPPh_3)_8]^{2+}$ (**1**) in good yield and $[(PPh_3)Pd(AuPPh_3)_6]^{2+}$ (**3**) as a minor product. These compounds were separated by HPLC methods. The structure of **1** was determined by single-crystal X-ray diffraction, and the $PdAu_8$ core has a palladium-centered crown or square-antiprismatic geometry similar to that of its Pt analogue.[2] Although a large number of transition-metal-gold phosphine cluster compounds have been prepared,[2-18] there exists a void of well-characterized cluster compounds that contain palladium and gold. In this paper we report an improved synthesis for **1** and **3** that gives the compounds separately and in high yield, as well as the synthesis and characterization of $[(CO)Pd(AuPPh_3)_8]^{2+}$ (**2**) and two new phosphite-containing cluster compounds $[(P(OCH_2)_3CCH_3)_2Pd(AuPPh_3)_6]^{2+}$ (**4**) and $[(P(OCH_3)_3Pd(AuPPh_3)_6(AuP(OCH_3)_3)_2]^{2+}$ (**5**). These compounds form a group of PdAu clusters that show novel structures and interesting reactivity and represent a significant advance in this research area.

The above cluster compounds are palladium centered and can be classified as having 16 or 18 Pd valence electrons. In electron counting for these complexes, the central Pd contributes 10 electrons, each $AuPPh_3$ or $AuP(OR)_3$ unit, 1 electron, and $P(OR)_3$ or CO, 2 electrons. This electron counting has been shown to be useful in predicting reactivity[2,14,15,18] and structure.[19,20] For example, the addition of CO to the 16-electron cluster **1** gives the stable 18-electron adduct **2**.[1] In this paper we show that compound **1** undergoes two reversible single-electron reductions by cyclic voltammetry to the neutral 18-electron cluster $[Pd(AuPPh_3)_8]^0$. A similar electrochemical result has been reported for the isoelectronic 16-electron clusters $[Pt(AuPPh_3)_8]^{2+}$ and $[Au(AuPPh_3)_8]^{3+}$,[21] and a comparison of the data will be made here. In this paper we also report the nucleophilic addition/substitution reactions of tertiary phosphites $P(OMe)_3$ and $P(OCH_2)_3CCH_3$ to the 16-electron clusters $Pd(AuPPh_3)_8^{2+}$ (**1**) and $[(PPh_3)Pd(AuPPh_3)_6]^{2+}$ (**3**), respectively, to give the new 18-electron com-

† Institute of Chemistry, University of São Paulo, São Paulo, Brazil.

(1) Ito, L. N.; Johnson, B. J.; Mueting, A. M.; Pignolet, L. H. *Inorg. Chem.* **1989**, *28*, 2026.
(2) Kanters, R. P. F.; Schlebos, P. P. J.; Bour, J. J.; Bosman, W. P.; Behm, H. J.; Steggerda, J. J. *Inorg. Chem.* **1988**, *27*, 4034. Bour, J. J.; Kanters, R. P. F.; Schlebos, P. P. J.; Bosman, W. P.; Behm, H.; Beurskens, P. T.; Steggerda, J. J. *Recl.: J. R. Neth. Chem. Soc.* **1987**, *106*, 157. Bour, J. J.; Kanters, R. P. F.; Schlebos, P. P. J.; Steggerda, J. J. *Recl.: J. R. Neth. Chem. Soc.* **1988**, *107*, 211.
(3) Mueting, A. M.; Bos, W.; Alexander, B. D.; Boyle, P. D.; Casalnuovo, J. A.; Balaban, S.; Ito, L. N.; Johnson, S. M.; Pignolet, L. H. In *Recent Advances in Di- and Polynuclear Chemistry*; Braunstein, P., Ed. *New J. Chem.* **1988**, *12*, 505 and references cited therein.
(4) Boyle, P. D.; Boyd, D. C.; Mueting, A. M.; Pignolet, L. H. *Inorg. Chem.* **1988**, *27*, 4424.
(5) Alexander, B. D.; Gomez-Sal, M. P.; Gannon, P. R.; Blaine, C. A.; Boyle, P. D.; Mueting, A. M.; Pignolet, L. H. *Inorg. Chem.* **1988**, *27*, 3301.
(6) Bos, W.; Steggerda, J. J.; Shiping, Y.; Casalnuovo, J. A.; Mueting, A. M.; Pignolet, L. H. *Inorg. Chem.* **1988**, *27*, 948.
(7) Boyle, P. D.; Johnson, B. J.; Alexander, B. D.; Casalnuovo, J. A.; Gannon, P. R.; Johnson, S. M.; Larka, E. A.; Mueting, A. M.; Pignolet, L. H. *Inorg. Chem.* **1987**, *26*, 1346.
(8) Smith, E. W.; Welch, A. J.; Treurnicht, I.; Puddephatt, R. J. *Inorg. Chem.* **1986**, *25*, 4616.
(9) Bour, J. J.; Kanters, R. P. F.; Schlebos, P. P. J.; Steggerda, J. J. *Recl. Trav. Chim. Pays-Bas* **1988**, *107*, 211.
(10) Bour, J. J.; Kanters, R. P. F.; Schlebos, P. P. J.; Bos, W.; Bosman, W. P.; Behm, H.; Beurskens, P. T.; Steggerda, J. J. *J. Organomet. Chem.* **1987**, *329*, 405.
(11) Jones, P. G. *Gold Bull.* **1986**, *19*, 46 and references cited therein.
(12) Braunstein, P.; Rosé, J. *Gold Bull.* **1985**, *18*, 17.
(13) Hall, K. P.; Mingos, D. M. P. *Prog. Inorg. Chem.* **1984**, *32*, 237 and references cited therein.
(14) Ito, L. N.; Felicissimo, A. M. P.; Pignolet, L. H. *Inorg. Chem.*, in press.
(15) Kanters, R. P. F.; Schlebos, P. P. J.; Bour, J. J.; Bosman, W. P.; Smits, J. M. M.; Beurskens, P. T.; Steggerda, J. J. *Inorg. Chem.* **1990**, *29*, 324.
(16) Bour, J. J.; Berg, W. V. D.; Schlebos, P. P.; Kanters, R. P. F.; Schoondergang, M. F. J.; Bosman, W. P.; Smits, J. M. M.; Beurskens, P. T.; Steggerda, J. J.; van der Sluis, P. *Inorg. Chem.* **1990**, *29*, 2971.
(17) Kanters, R. P. F.; Bour, J. J.; Schlebos, P. P. J.; Steggerda, J. J. *J. Chem. Soc., Chem. Commun.* **1988**, 1634.
(18) Ito, L. N.; Sweet, J. D.; Mueting, A. M.; Pignolet, L. H.; Schoondergang, M. F. J.; Steggerda, J. J. *Inorg. Chem.* **1989**, *28*, 3696.
(19) Stone, A. J. *Inorg. Chem.* **1981**, *20*, 563.

0020-1669/91/1330-0988$02.50/0

pounds **5** and **4**. X-ray crystal structures are reported on clusters **2** and **5**, and their cluster core geometries are in agreement with predictions based on electron counting.[2,14,17-19] Compound **2** is a rare example of a metal cluster that contains a CO ligand that is terminally bonded to a Pd atom.

Experimental Section

Physical Measurements and Reagents. ^{31}P NMR spectra were recorded at 121.5 MHz with use of a Nicolet NT-300 or a Varian VXR-300 MHz spectrometer and at 202.3 MHz with use of a Varian VXR-500 NMR spectrometer; ^{1}H NMR spectra were recorded at 300 MHz with use of a Varian VXR-300 MHz spectrometer. ^{31}P NMR spectra were run with proton decoupling, and spectra are reported in ppm relative to internal standard trimethyl phosphate (TMP), with positive shifts downfield. ^{1}H NMR spectra are reported in ppm relative to external standard tetramethylsilane (TMS), with positive shifts downfield. Infrared spectra were recorded on a Perkin-Elmer 1710 FT-IR spectrometer. Conductivity measurements were made with use of a Yellow Springs Model 31 conductivity bridge. Compound concentrations used in the conductivity experiments were 3×10^{-4} M in CH_3CN. FABMS experiments were carried out with use of a VG Analytical, Ltd., 7070E-HF high-resolution double-focusing mass spectrometer equipped with a VG 11/250 data system.[3,7] Microanalyses were carried out by Analytische Laboratorien, Engelskirchen, West Germany. Solvents were dried and distilled prior to use. $Pd(PPh_3)_4$,[22] $P(OCH_2)_3CCH_3$,[23] and $Au(PPh_3)NO_3$[24] were prepared as described in the literature. $Pd(acetate)_2$ was purchased from Aldrich Chemical Co. and used as received. All manipulations were carried out under a purified N_2 atmosphere with use of standard Schlenk techniques unless otherwise noted.

Electrochemical measurements were performed as described previously[21] at the Department of Inorganic Chemistry, University of Nijmegen, The Netherlands, by using a PAR Model 173 potentiostat equipped with a PAR Model 176 I/E converter coupled to a PAR Model 175 universal programmer. Platinum working and auxiliary electrodes were used. In CH_2Cl_2 solutions a SSCE reference electrode was used, and in CH_3CN a Ag/Ag^+ (0.1 M $AgNO_3$) reference electrode was used. Solutions of both solvents contained 0.1 M n-Bu_4NPF_6 as supporting electrolyte. The half-wave potentials for 10^{-3} M solutions of the ferrocene/ferrocenium redox couple were measured under identical experimental conditions: $E_{1/2} = 0.422$ V (CH_2Cl_2) vs SSCE; $E_{1/2} = 0.071$ V (CH_3CN) vs Ag/Ag^+. Cyclic voltammetric data are reported for a scan rate of 100 mV/s, and differential pulse polarography, for a scan rate of 5 mV/s with a pulse amplitude of 10 mV.

Preparation of Compounds. $[Pd(AuPPh_3)_8](NO_3)_2$ ($1(NO_3)_2$). The preparation of this compound has been previously communicated by us,[1] but the method reported below gives a better yield and more importantly does not require the use of HPLC. This new method is therefore the one of choice. A 100-mL Schlenk flask was charged with $Pd(PPh_3)_4$ (220 mg, 1.90×10^{-1} mmol), $Au(PPh_3)NO_3$ (794 mg, 1.52 mmol), and a magnetic stir bar. Dichloromethane (40 mL) was added to the reaction vessel, and a dark red homogeneous solution resulted. A methanol solution of $NaBH_4$ (30 mL, 40 mg, 1.06 mmol) was added to the magnetically stirred reaction mixture, during which time gas evolution occurred. The dark brown solution was stirred at ambient temperature for 10 min, at which time water (1 mL) was added to the reaction mixture to quench the reaction. The solvents were removed under vacuum. Methanol (20 mL) was added to the flask and the crude mixture filtered through a bed of diatomaceous earth on a fritted glass filter. The dark brown filtrate was evaporated to dryness. The brown solid was dissolved in acetone (10 mL) and the solution filtered through a bed of diatomaceous earth on a fritted glass filter. The solvent was removed under vacuum, leaving a dark purple solid. Crystals of the nitrate salt of **1** were grown by dissolving the crude solid in a minimal amount of methanol and adding diethyl ether in small portions, with mixing of the solution, until a small amount of a fine microcrystalline precipitate formed. The flask was left undisturbed overnight, during which time platey, dark purple crystals formed. Yield: 432 mg (58%, based on Au, after recrystallization). $1(NO_3)_2$ is soluble in alcohols, dichloromethane, chloroform, and acetone, is insoluble in saturated hydrocarbons and diethyl ether, and is air, light, and moisture stable both in the solid state and in solution. The PF_6^- salt of **1** was made by dissolving $1(NO_3)_2$ (50 mg, 0.0128 mmol) in methanol (2 mL) and adding the solution dropwise to a stirred solution containing NH_4PF_6 (21 mg, 0.129 mmol) in methanol (10 mL). Immediately upon mixing, a brown precipitate formed, which was then collected on a fritted glass filter, washed with methanol (10 mL), and dried under vacuum. ^{31}P NMR (CH_2Cl_2, 25 °C): δ 48.8 (s). The conductance of $1(PF_6)_2$ (166.2 cm^2 mhos mol^{-1}) is indicative of a 1:2 electrolyte in CH_3CN solution. FABMS and elemental analysis of this compound have been reported previously.[1]

$[(CO)Pd(AuPPh_3)_8](NO_3)_2$ ($2(NO_3)_2$) was prepared by dissolving complex $1(NO_3)_2$ (100 mg, 2.56×10^{-2} mmol) in dichloromethane (10 mL) and placing the solution under 1 atm of CO. The color of the solution changed from purple to dark brown immediately. The volume of the solution was reduced to 2 mL under a CO purge and transferred to a magnetically stirred flask containing diethyl ether (60 mL) saturated with CO. The brown precipitate was collected on a fritted filter, washed with diethyl ether (40 mL), and dried under vacuum. Yield: 98 mg (97%). Crystals of $2(NO_3)_2$ were grown by dissolving the solid in a minimal amount of methanol and adding diethyl ether in small portions, with mixing of the solution, until a small amount of a fine microcrystalline precipitate formed. The flask was left undisturbed overnight, during which time black crystals formed. All of these manipulations were done under 1 atm of CO. $2(NO_3)_2$ is soluble in alcohols, dichloromethane, chloroform, and acetone, is insoluble in saturated hydrocarbons and diethyl ether, and is air, light, and moisture stable both in the solid state and in solution. Solution samples should be kept under 1 atm of CO as this ligand is labile and can be lost from the compound forming **1**. The isotopically labeled analogue, $[(^{13}CO)Pd(AuPPh_3)_8](NO_3)_2$, was prepared by the same procedure with ^{13}CO. ^{31}P NMR (CH_2Cl_2, 25 °C): δ 44.5 (s). ^{13}C NMR (CD_2Cl_2, 25 °C): δ 229.7 (m, $J_{^{13}C-P} = 11.7$ Hz). IR (KBr): ν(CO) 1955 cm^{-1}, $\nu(^{13}CO)$ 1919 cm^{-1} [$\nu(CO)/\nu(^{13}CO) = 1.019$], $\nu(NO_3)$ 1343 cm^{-1}. IR (CH_2Cl_2 solution): 1968 cm^{-1}. The equivalent conductance (162.1 cm^2 mhos mol^{-1}) is indicative of a 1:2 electrolyte in CH_3CN solution.

$[(PPh_3)Pd(AuPPh_3)_6](NO_3)_2$ ($3(NO_3)_2$). The preparation of this compound was communicated previously by us,[1] but the method given below gives a much better yield and does not require the use of HPLC. This new procedure is therefore the one of choice. $3(NO_3)_2$ is prepared by dissolving $Pd(acetate)_2$ (24 mg, 0.107 mmol) and PPh_3AuNO_3 (75 mg, 0.144 mmol) in CH_2Cl_2 (20 mL) and magnetically stirring the solution under 1 atm of H_2. After 17 h the volume of the solution was reduced under vacuum to approximately 10 mL and Et_2O added to precipitate a brown solid. The solid was isolated on a fritted glass filter, washed with Et_2O, and dried under vacuum. Yield: 59 mg (87% based on Au). $3(NO_3)_2$ is soluble in CH_2Cl_2, chloroform, alcohols, and acetone, is insoluble in saturated hydrocarbons and Et_2O, and is air, light, and moisture stable both in the solid state and in solution. Crystals of the mixed salt $3(NO_3,PF_6)$ were obtained by the addition of 2 equiv of NH_4PF_6 to a MeOH solution containing $3(NO_3)_2$ followed by slow evaporation of the solvent until the initiation of crystallization. IR spectroscopy showed the presence of both counterions ($\nu(NO_3)$ = 1343 cm^{-1} and $\nu(PF_6)$ = 839 cm^{-1}). ^{31}P NMR (CD_2Cl_2, 20 °C): δ 59.8 (septet, $^3J_{P-P} = 31$ Hz, int = 1), 47.5 (d, $^3J_{P-P} = 31$ Hz, int = 6). FABMS (*m*-nitrobenzyl alcohol matrix): m/z 3267 ($[(PPh_3)Pd(AuPPh_3)_6(PF_6)]^+ = M^+$), 3005 ($(M - PPh_3)^+$), 2860 ($(M - PPh_3 - PF_6)^+$). IR: $\nu(NO_3)$ 1343 cm^{-1}. The equivalent conductance (184.7 cm^2 mhos mol^{-1}) is indicative of a 1:2 electrolyte in CH_3CN solution. Anal. Calcd for $3(NO_3,PF_6)$, $Au_6PdP_8C_{126}H_{105}F_6NO_3$: C, 45.43; H, 3.18; P, 7.44. Found: C, 45.97; H, 3.19; P, 7.59.

$[(P(OCH_2)_3CCH_3)_2Pd(AuPPh_3)_6](NO_3)_2$ ($4(NO_3)_2$) was prepared by dissolving $3(NO_3)_2$ (50 mg, 0.015 mmol) in CH_2Cl_2 (2 mL), in a Schlenk tube, and adding $P(OCH_2)_3CCH_3$ (5 mg, 0.0338 mmol) to the reaction vessel. The color of the solution changed immediately from brown to purple. Crystals of the nitrate salt of **4** were grown by adding diethyl ether in small portions, with mixing of the solution, until a small amount of a fine microcrystalline precipitate formed. The flask was left undisturbed overnight, during which time purple crystals formed. Yield: 41 mg (81%). $4(NO_3)_2$ is soluble in alcohols, dichloromethane, chloroform, and acetone, is insoluble in saturated hydrocarbons and diethyl ether, and is air, light, and moisture stable both in the solid state and in solution. ^{31}P NMR (CD_2Cl_2, 21 °C): δ 185.1 (septet, $^3J_{P-P} = 55.5$ Hz, int = 1), 44.3 (t, $^3J_{P-P} = 55.5$ Hz, int = 3). ^{1}H NMR (CD_2Cl_2, 20 °C): δ 7.4–6.6 (m, phenyl H's, int = 15), 3.43 (s, OCH_2, int = 2), 0.40 (s, CCH_3, int = 1). FABMS (*m*-nitrobenzyl alcohol matrix): m/z 3219 [$((P(OCH_2)_3CCH_3)_2Pd(AuPPh_3)_6(NO_3)]^+ = M^+$), 3005 ($(M - P(OCH_2)_3CCH_3 - NO_3)^+$), 2922 ($(M - 2P(OCH_2)_3CCH_3)^+$), 2808 ($(M - P(OCH_2)_3CCH_3 - PPh_3)^+$). IR (KBr): $\nu(NO_3)$ 1343 cm^{-1}. The equivalent conductance (181 cm^2 mhos mol^{-1}) is indicative of a 2:1 electrolyte in CH_3CN solution.

$[(P(OCH_3)_3)Pd(AuPPh_3)_6(AuP(OCH_3)_3)_2](NO_3)_2$ ($5(NO_3)_2$) was prepared by dissolving $1(NO_3)_2$ (50 mg, 0.0128 mmol) in MeOH (2 mL)

(20) Mingos, D. M. P.; Johnston, R. L. *Struct. Bonding* **1987**, *68*, 29.
(21) Van der Linden, J. G. M.; Roelofsen, A. M.; Ipskamp, G. H. W. *Inorg. Chem.* **1989**, *28*, 967. Van der Linden, J. G. M.; Paulissen, M. L. H.; Schmitz, J. E. J. *J. Am. Chem. Soc.* **1983**, *105*, 1903.
(22) Coulson, D. R. *Inorg. Synth.* **1972**, *13*, 121.
(23) Verkade, J. G.; Piper, T. S. *Inorg. Chem.* **1963**, *2*, 944.
(24) Malatesta, L.; Naldini, L.; Simonetta, G.; Cariati, F. *Coord. Chem. Rev.* **1966**, *1*, 255.

Table I. Crystallographic Data for $[(CO)Pd(AuPPh_3)_8](NO_3)_2\cdot(CH_3CH_2)_2O$ ($2(NO_3)_2\cdot(CH_3CH_2)_2O$) and $[(P(OMe)_3)Pt(AuPPh_3)_6(AuP(OMe)_3)_2](NO_3)_2$ ($5(NO_3)_2$)

	$2(NO_3)_2\cdot(CH_3CH_2)_2O$	$5(NO_3)_2$
Crystal Parameters and Measurement of Intensity Data		
space group	$P\bar{1}$ (No. 2)	$P\bar{1}$ (No. 2)
cell params at T, °C	−85	24
a, Å	16.23 (1)	18.577 (3)
b, Å	16.94 (2)	19.248 (3)
c, Å	30.78 (1)	21.963 (8)
α, deg	89.63 (6)	82.00 (2)
β, deg	87.61 (5)	78.16 (2)
γ, deg	62.54 (7)	74.90 (2)
V, Å^3	7496	7390
Z	2	2
calcd density, g cm^{-3}	1.884	1.688
abs coeff, cm^{-1}	80.2	81.5
max, min transm factors	0.98, 0.62	1.39, 0.66
formula	$C_{149}H_{130}N_2O_8P_8Au_8Pd$	$C_{117}H_{117}N_2O_{15}P_9Au_8Pd$
fw	4006.59	3756.11
radiation (λ, Å)	Mo Kα graphite monochromatized (0.71069)	
Refinement by Full Matrix Least Squares		
R^a	0.075	0.060
$R_w{}^a$	0.085	0.069

[a] The function minimized was $\sum w(|F_o| - |F_c|)^2$, where $w = 4F_o^2/\sigma^2(F_o)^2$. The unweighted and weighted residuals are defined as $R = \sum(||F_o| - |F_c||)/\sum|F_o|$ and $R_w = [(\sum w(|F_o| - |F_c|)^2)/(\sum w|F_o|^2)^{1/2}$.

in a Schlenk tube and adding $P(OCH_3)_3$ (6 μL, 0.0509 mmol) to the reaction vessel. The color of the solution changed immediately from brown to black. Crystals were prepared by adding diethyl ether in small portions, with mixing of the solution, until a small amount of a fine microcrystalline precipitate formed. The flask was left undisturbed overnight, during which time black crystals formed. The crystals were isolated on a fritted glass filter, washed with Et_2O (10 mL), and dried under vacuum. Yield: 37 mg (77%). $5(NO_3)_2$ is soluble in alcohols, CH_2Cl_2, chloroform, and acetone, is insoluble in saturated hydrocarbons and Et_2O, and is air, light, and moisture stable both in the solid state and in solution. The BF_4^- salt of **5** was prepared by dissolving $5(NO_3)_2$ in a minimal amount of MeOH and adding the solution to a saturated MeOH solution of NH_4BF_4. The brown precipitate was isolated on a fritted glass filter, washed with Et_2O, and dried under vacuum. ^{31}P NMR (CD_2Cl_2, 20 °C): δ 227.3 (s (br), int = 1), 156.1 (s (br), int = 2), 45.0 (s (br), int = 6); at −90 °C nine multiplet resonances with int = 1 were observed at δ 228.1, 157.8, 149.4, 48.7, 47.7, 44.2, 41.8, 38.9, and 36.3. FABMS of $5(BF_4)_2$ (*m*-nitrobenzyl alcohol matrix): *m/z* 3802 ($[[P(OCH_3)_3)Pd(AuPPh_3)_6(AuP(OCH_3)_3)_2(BF_4)]^+ = M^+$), 3591 ((M − $P(OCH_3)_3$) − $BF_4)^+$), 2453 ((M − PPh_3 − $BF_4)^+$), 3329 ((M − $P(OCH_3)_3$) − PPh_3 − $BF_4)^+$). IR: $\nu(NO_3)$ 1343 cm^{-1}. The equivalent conductance (171.2 cm^2 mhos mol^{-1}) is indicative of a 1:2 electrolyte in CH_3CN solution. Anal. Calcd for $5(NO_3)_2$, $Au_8PdP_9C_{117}H_{117}N_2O_{15}$: C, 37.45; H, 3.14; P, 7.43. Found: C, 36.63; H, 2.88; P, 6.86.

X-ray Structure Determinations. Collection and Reduction of X-ray Data. A summary of crystal data is presented in Table I. Crystals of both compounds rapidly lost solvent and fragmented upon removal from the crystallizing solution. A crystal of $[(CO)Pd(AuPPh_3)_8](NO_3)_2\cdot(CH_3CH_2)_2O$ ($2(NO_3)_2\cdot(CH_3CH_2)_2O$) was coated with a viscous high molecular weight hydrocarbon and secured on a glass fiber by cooling in a cold N_2 stream on the diffractometer. A crystal of $[(P(OCH_3)_3)Pd(AuPPh_3)_6(AuP(OCH_3)_3)_2](NO_3)_2$ ($5(NO_3)_2$) was sealed inside a glass capillary tube that contained some of the crystallizing solution. These techniques were necessary to stabilize the crystals for data collection. The crystal classes and space groups were unambiguously determined by the Enraf-Nonius CAD4 peak search, centering, and indexing programs[25] and by successful solution and refinement of the structures (vide infra). The intensities of three standard reflections were measured every 1.5 h of X-ray exposure time during data collection, and no decay was noted for either crystal. The data were corrected for Lorentz, polarization, and background effects. An empirical absorption correction was applied by use of the program DIFABS.[26] All data were collected by using an Enraf-Nonius CAD-4 diffractometer with controlling hardware and software,[25] and all calculations were performed by using the Molecular Structure Corp. TEXSAN crystallographic software package,[27] run on a Microvax 3 computer.

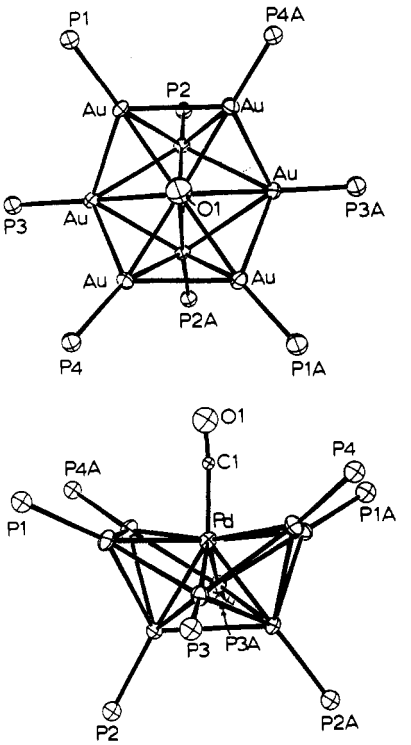

Figure 1. ORTEP drawings of the coordination core of **2**. Ellipsoids are drawn with 50% probability boundaries, and phenyl rings have been omitted for clarity. The Au atoms have the same labels as the P atoms to which they are attached.

Solution and Refinement of the Structures. Both structures were solved by direct methods.[28,29] Full-matrix least-squares refinement and difference Fourier calculations were used to locate most of the remaining non-hydrogen atoms. The nitrate counterions were not located for either crystal, and there were signs of disordered solvent molecules in the difference Fourier maps near the end of the refinement. In the case of $2(NO_3)_2$, one diethyl ether solvate molecule was located and refined satisfactorily. Since none of the other peaks located refined well or made any chemical sense, they were omitted from the structure determination. In addition, four of the nine trimethyl phosphite carbon atoms in $5(NO_3)_2$ could not be located due to disorder. Disorder in ligands, solvent molecules, and counterions is common in structures of metal cluster compounds of this type and is not believed to significantly affect the molecular dimensions of the metal framework. The atomic scattering factors were taken from the usual tabulation,[30] and the effects of anomalous dispersion were included in F_c by using Cromer and Ibers's values of $\Delta f'$ and $\Delta f''$.[31] The metal and phosphorus atoms in $5(NO_3)_2$ and the metal atoms in $2(NO_3)_2\cdot(CH_3CH_2)_2O$ were refined with anisotropic thermal parameters. The phenyl carbon atoms in $5(NO_3)_2$ were refined as rigid groups. When the structure of $5(NO_3)_2$ was refined by using all of the data (0–40° in 2θ), refinement converged with $R = 0.11$. Inspection of the results suggested the first data shell collected, the low-angle data from 0 to 13°, were not good data. When these data were omitted and only the higher angle data used, $R = 0.060$. The crystal was probably moving in the capillary tube and settled down after this first low-angle shell was completed. Since the parameters for both refinements were essentially the same and the crystal was lost at the end of data collection, it was decided to report the results using only the higher angle data. The positions of the hydrogen atoms in the PPh_3 ligands were not included

(25) Schagen, J. D.; Straver, L.; van Meurs, F.; Williams, G. Enraf-Nonius Delft, Scientific Instruments Division, Delft, The Netherlands, 1988.
(26) Walker, N.; Stuart, D. *Acta Crystallogr., Sect. A* **1983**, *A39*, 158.
(27) All calculations on the analysis of **2** were carried out with the use of the Molecular Structure Corp. TEXSAN-TEXRAY Structure Analysis Package, version 2.1, 1985.
(28) MITHRIL (an integrated direct methods computer program; University of Glascow, Scotland): Gilmore, C. J. *J. Appl. Crystallogr.* **1984**, *17*, 42.
(29) DIRDIF (direct methods for difference structures; an automatic procedure for phase extension and refinement of difference structure factors): Beurskens, P. T. Technical Report 1984/1; Crystallography Laboratory: Toernooiveld, 6525 Ed. Nijmegen, The Netherlands.
(30) Cromer, D. T.; Waber, J. T. In *International Tables for X-Ray Crystallography*; Kynoch: Birmingham, England, 1974; Vol. IV, Table 2.2.4.
(31) Cromer, D. T. In *International Tables for X-Ray Crystallography*; Kynoch: Birmingham, England, 1974; Vol. IV, Table 2.3.1.

Table II. Positional Parameters and Their Estimated Standard Deviations for Core Atoms in $[(CO)Pd(AuPPh_3)_8](NO_3)_2 \cdot (CH_3CH_2)_2O$

atom	x	y	z	B, Å²
Au1	0.5258 (1)	0.5670 (1)	0.31905 (5)	1.7 (1)
Au2	0.4258 (1)	0.6373 (1)	0.24105 (5)	1.5 (1)
Au3	0.5872 (1)	0.4518 (1)	0.24549 (5)	1.5 (1)
Au4	0.7431 (1)	0.4647 (1)	0.21098 (5)	1.7 (1)
Au1A	0.6839 (1)	0.6454 (1)	0.17872 (5)	1.6 (1)
Au2A	0.5671 (1)	0.5649 (1)	0.16925 (5)	1.4 (1)
Au3A	0.4931 (1)	0.7582 (1)	0.20318 (5)	1.6 (1)
Au4A	0.4862 (1)	0.7448 (1)	0.29511 (5)	1.8 (1)
Pd	0.5993 (2)	0.6061 (2)	0.2467 (1)	1.3 (2)
P1	0.5140 (7)	0.5362 (6)	0.3910 (4)	1.8 (2)*
P2	0.2759 (7)	0.6617 (6)	0.2334 (4)	1.7 (2)*
P3	0.6011 (7)	0.3122 (6)	0.2536 (4)	1.9 (2)*
P4	0.8909 (7)	0.3521 (6)	0.2080 (4)	1.8 (2)*
P1A	0.7798 (7)	0.6950 (7)	0.1433 (4)	2.3 (2)*
P2A	0.5381 (7)	0.5353 (6)	0.1011 (3)	1.7 (2)*
P3A	0.4212 (7)	0.9003 (7)	0.1737 (4)	2.2 (2)*
P4A	0.4416 (7)	0.8546 (6)	0.3469 (3)	1.7 (2)*
C1	0.693 (2)	0.612 (2)	0.279 (1)	0.7 (6)*
O1	0.742 (2)	0.617 (2)	0.300 (1)	3.2 (6)*

[a] Counterion, solvent molecule, and phenyl group positional parameters are provided in the supplementary material. Starred B values are for atoms that were refined isotropically. B values for anisotropically refined atoms are given in the form of the isotropic equivalent thermal parameter defined as $(4/3)[a^2\beta(1,1) + b^2\beta(2,2) + c^2\beta(3,3) + ab(\cos\gamma)\beta(1,2) + ac(\cos\beta)\beta(1,3) + bc(\cos\alpha)\beta(2,3)]$.

Table III. Positional Parameters and Their Estimated Standard Deviations for Core Atoms in $[(P(OCH_3)_3)Pd(AuPPh_3)_6(AuP(OCH_3)_3)_2](NO_3)_2$ ($\mathbf{5}(NO_3)_2$)[a]

atom	x	y	z	B, Å²
Au1	0.8748 (1)	0.30447 (8)	0.09944 (7)	2.5 (1)
Au1A	0.8183 (1)	0.35944 (9)	0.33994 (7)	2.7 (1)
Au2	0.8138 (1)	0.20623 (8)	0.19455 (8)	2.7 (1)
Au2A	0.7186 (1)	0.29138 (9)	0.29251 (8)	2.7 (1)
Au3	0.7237 (1)	0.35402 (9)	0.15851 (8)	2.9 (1)
Au3A	0.8725 (1)	0.21321 (8)	0.31011 (7)	2.7 (1)
Au4	0.7254 (1)	0.43924 (9)	0.25240 (8)	3.2 (1)
Au4A	0.9654 (1)	0.21648 (9)	0.18899 (8)	2.7 (1)
Pd	0.8431 (2)	0.3269 (2)	0.2210 (1)	1.8 (2)
P1	0.9205 (7)	0.3040 (6)	−0.0066 (5)	2.6 (7)
P1A	0.8173 (7)	0.4061 (7)	0.4313 (5)	3.6 (8)
P2	0.7748 (8)	0.1104 (6)	0.1778 (6)	3.5 (8)
P2A	0.6155 (7)	0.2501 (6)	0.3433 (6)	3.6 (8)
P3	0.6325 (7)	0.3994 (6)	0.0973 (6)	3.4 (8)
P3A	0.9119 (7)	0.1278 (6)	0.3895 (5)	3.1 (8)
P4	0.640 (1)	0.5450 (7)	0.2702 (7)	4 (1)
P4A	1.0882 (7)	0.1479 (6)	0.1589 (5)	3.4 (8)
P9	0.9211 (7)	0.4051 (6)	0.1973 (5)	2.9 (7)

[a] Counterion, solvent molecule, and phenyl group positional parameters are provided in the supplementary material. Starred B values are for atoms that were refined isotropically. B values for anisotropically refined atoms are given in the form of the isotropic equivalent thermal parameter defined as $(4/3)[a^2\beta(1,1) + b^2\beta(2,2) + c^2\beta(3,3) + ab(\cos\gamma)\beta(1,2) + ac(\cos\beta)\beta(1,3) + bc(\cos\alpha)\beta(2,3)]$.

in the structure factor calculations of either structure. The final positional and thermal parameters of the refined atoms within the coordination core for $\mathbf{2}(NO_3)_2$ and $\mathbf{5}(NO_3)_2$ are given in Tables II and III, respectively. ORTEP drawings of the cluster cores for both compounds including the labeling schemes are shown in Figures 1 and 2. Table IV gives selected distances and angles within the cluster cores of complexes **2** and **5**. A complete listing of crystallographic data, thermal and positional parameters, distances, angles, and structure factor amplitudes are included as supplementary material.[32]

Results

The transformations observed in this study are summarized in Scheme I. All of the compounds listed were isolated as solids in high yield. The spectroscopic and crystallographic data obtained for the compounds are given in the Experimental Section and

(32) See paragraph at end of the paper regarding supplementary material.

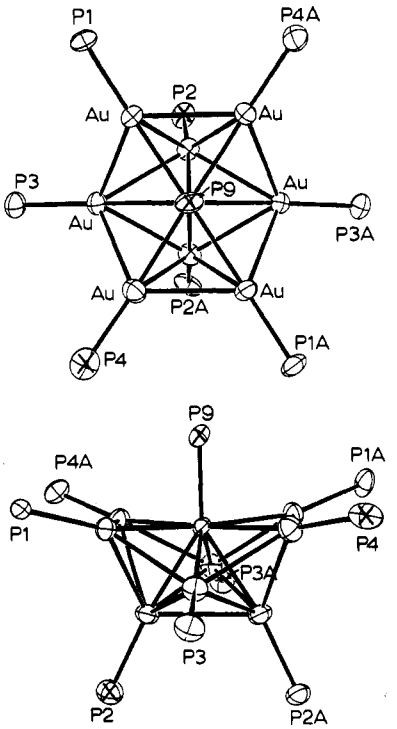

Figure 2. ORTEP drawings of the coordination core of **5**. Ellipsoids are drawn with 50% probability boundaries, and phenyl rings and OCH_3 groups have been omitted for clarity. The Au atoms have the same labels as the P atoms to which they are attached. The three phosphite P atoms are marked with an X.

Scheme I

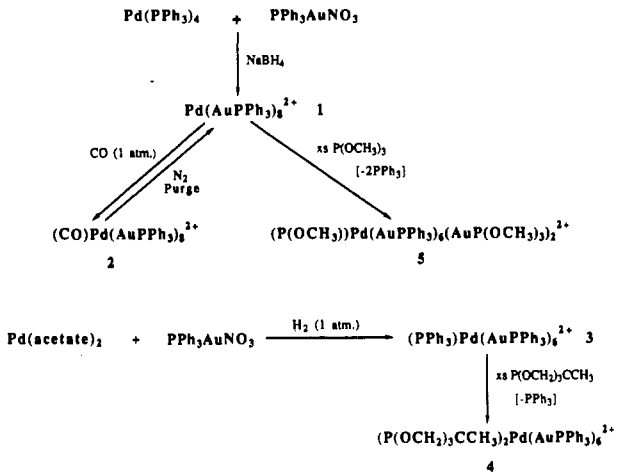

Tables I–IV and are discussed in the next section. The results of the electrochemical analysis of **1** are presented in Table V.

Discussion

Synthesis and Spectroscopic Characterization of the Clusters. Values of NMR coupling constants and chemical shifts are given in the Experimental Section and therefore are not generally repeated in this section. Refer to Scheme I for the formulation of the compounds and for a summary of their transformations. Improved syntheses have been developed for complexes $[Pd(AuPPh_3)_8]^{2+}$ (**1**) and $[(PPh_3)Pd(AuPPh_3)_6]^{2+}$ (**3**). The previous method required the use of HPLC separation of these two clusters, which were produced simultaneously.[1] The new synthesis of **1** is similar to the old one in that a mixture of $Pd(PPh_3)_4$ and PPh_3AuNO_3 is reduced by $NaBH_4$ but with different relative amounts of reactants. Since **1** has been well-characterized previously including a single-crystal X-ray analysis, no discussion is needed here.[1]

The 16-electron compound **1** has been shown to add one CO ligand, giving the 18-electron compound $[(CO)Pd(AuPPh_3)_8]^{2+}$

Table IV. Selected Bond Lengths (Å) and Bond Angles (deg) with Esd's for the Cluster Cores of **2** and **5**[a]

	2	5		2	5
Pd-Au1	2.705 (4)	2.684 (4)	Au1-Au3	2.827 (3)	2.817 (2)
Pd-Au1A	2.699 (4)	2.691 (4)	Au1-Au4A	2.873 (4)	2.918 (3)
Pd-Au4	2.653 (5)	2.694 (3)	Au3-Au4	2.804 (3)	2.818 (3)
Pd-Au4A	2.634 (4)	2.724 (3)	Au4-Au1A	2.932 (4)	2.861 (3)
Pd-Au2	2.628 (4)	2.682 (4)	Au1A-Au3A	2.855 (4)	2.852 (2)
Pd-Au2A	2.628 (1)	2.705 (4)	Au3A-Au4A	2.839 (3)	2.861 (2)
Pd-Au3	2.711 (6)	2.743 (4)	Au1-Au2	2.884 (3)	2.876 (2)
Pd-Au3A	2.727 (4)	2.747 (3)	Au2-Au4A	2.979 (3)	2.851 (3)
Au1-P1	2.29 (1)	2.31 (1)	Au2A-Au1A	2.825 (3)	2.943 (3)
Au1A-P1A	2.32 (1)	2.30 (1)	Au2A-Au4	2.912 (4)	2.887 (2)
Au4-P4	2.27 (1)	2.26 (1)	Au2-Au3	3.027 (4)	2.993 (2)
Au4A-P4A	2.28 (1)	2.33 (1)	Au2-Au3A	2.946 (3)	2.993 (3)
Au2-P2	2.29 (1)	2.25 (2)	Au2A-Au3	2.951 (3)	3.014 (3)
Au2A-P2A	2.28 (1)	2.28 (1)	Au2A-Au3A	3.091 (4)	2.939 (3)
Au3-P3	2.28 (1)	2.30 (1)	Au2-Au2A	2.943 (3)	2.890 (2)
Au3A-P3A	2.33 (1)	2.32 (1)	Pd-C1	1.90 (3)	
Pd-P9		2.29 (1)	C1-O1	1.07 (4)	
	2	**5**		**2**	**5**
Au1-Pd-Au1A	175.1 (1)	174.6 (2)	Au2-Pd-Au1	65.5 (1)	64.82 (9)
Au4-Pd-Au4A	166.3 (1)	177.9 (2)	Au2-Pd-Au4A	69.0 (1)	63.65 (9)
Au1-Pd-Au4	112.9 (1)	115.0 (1)	Au2A-Pd-Au1A	64.0 (1)	66.12 (9)
Au1A-Pd-Au4A	114.3 (1)	115.3 (1)	Au2A-Pd-Au4	66.9 (1)	64.66 (8)
Au1-Pd-Au4A	65.1 (5)	65.30 (8)	Au2-Pd-Au2A	68.1 (1)	64.9 (1)
Au1A-Pd-Au4	66.4 (1)	64.19 (8)	P9/C1-Pd-Au1	91 (1)	87.4 (3)
Au3-Pd-Au1	62.9 (1)	62.53 (9)	P9/C1-Pd-Au1A	84 (1)	87.2 (3)
Au3-Pd-Au4	63.0 (1)	62.43 (9)	P9/C1-Pd-Au4	83 (1)	88.9 (3)
Au3-Pd-Au2	69.1 (9)	67.0 (1)	P9/C1-Pd-Au4A	84 (1)	89.0 (3)
Au3-Pd-Au2A	67.1 (3)	67.2 (1)	P9/C1-Pd-Au3	119 (1)	117.4 (3)
Au3A-Pd-Au1A	63.5 (1)	63.25 (8)	P9/C1-Pd-Au3A	114 (1)	118.9 (3)
Au3A-Pd-Au4A	63.9 (1)	63.07 (8)	P9/C1-Pd-Au2	149 (1)	146.8 (3)
Au3A-Pd-Au2	66.7 (1)	66.90 (9)	P9/C1-Pd-Au2A	142 (1)	148.3 (3)
Au3A-Pd-Au2A	70.5 (1)	65.24 (8)	Pd-Au1-P1	157.0 (3)	166.3 (3)
Pd-Au2-P2	177.6 (3)	173.1 (3)	Pd-Au3-P3	168.5 (3)	167.4 (4)
Pd-Au4-P4	154.8 (3)	170.5 (4)	Pd-Au1A-P1A	157.3 (3)	165.5 (4)
Pd-Au2A-P2A	177.4 (3)	172.1 (3)	Pd-Au3A-P3A	167.5 (3)	169.9 (4)
Pd-Au4A-P4A	158.1 (3)	163.7 (4)	Pd-C1-O1	176 (3)	

[a] Values for the two compounds are listed for equivalent distances and angles to facilitate a comparison of the two structures.

Table V. Comparison of $[M(AuPPh_3)_8]^{2+}$ (M = Pd, Pt, Au) Potentials[a]

cluster	solvent	$E_{1/2}(1)$, V	$E_{1/2}(2)$, V	$\Delta E_{1/2}$, V[b]	ref
$Pd(AuPPh_3)_8^{2+}$	CH_2Cl_2	−1.80	−1.98	0.147	this work
$Pt(AuPPh_3)_8^{2+}$	CH_2Cl_2	−1.57	−1.72	0.147	*c*
$Au(AuPPh_3)_8^{2+}$	CH_2Cl_2	−1.03	−1.11	0.084	*c*
$Pd(AuPPh_3)_8^{2+}$	CH_3CN	−1.70	−1.76	0.076	this work
$Pt(AuPPh_3)_8^{2+}$	CH_3CN	−1.53	−1.59	0.065	*c*

[a] Potentials vs $[Fe(C_5H_5)_2]^{+,0}$ redox couple. [b] Values for $\Delta E_{1/2}$ measured by DPP. [c] Reference 21.

(**2**). This addition is reversible as the CO is readily removed by an N_2 purge. This is in contrast to the Pt analogue, $[(CO)Pt(AuPPh_3)_8]^{2+}$, in which case the CO is not removed by an N_2 purge.[2] The spectroscopic data of **2** are consistent with its formulation. Most noteworthy is a comparison of IR (KBr) and ^{13}C NMR data for **2** and its Pt analogue[2] (ν(CO) = 1955 and 1940 cm^{-1}; $\delta(^{13}C)$ = 230 and 211 ppm, respectively). The higher CO stretching frequency, which indicates less back-bonding, for **2** is consistent with its increased lability relative to the Pt-centered compound. These spectroscopic data suggest that the CO ligand is terminally bonded to Pd by analogy to the Pt analogue, which was characterized by X-ray diffraction.[2] The CO stretching frequency for the Pt-centered cluster is at the lower end of the range found for terminal CO in homonuclear platinum carbonyl cluster compounds of the type $[Pt_3(CO)_6]_n^{2-}$[33] and suggests that the Pt is unusually electron rich. Carbonyl cluster compounds of Pd are almost always found with bridging CO ligands and have CO stretching frequencies in the 1934–1975-cm^{-1} range, whereas mononuclear terminally bonded palladium carbonyls have values much higher than the 1955 cm^{-1} value (or 1968 cm^{-1} in CH_2Cl_2 solution) observed in **2**. The only known metal cluster that has a CO ligand terminally bonded to a Pd atom is $[Pd_2Co(CO)_4(dppm)_2]^+$.[34] This compound has a very high CO stretching frequency of 2070 cm^{-1} and also shows reversible CO dissociation.[34] It is therefore not possible to unambigously determine the CO bonding mode in **2** by IR data alone. The ^{13}C chemical shifts for the CO ligands in **2** and its Pt analogue are also unusual in that they appear very far down field compared with values of known terminally bonded Pt and Pd carbonyls.[35] We have no good explanation for this, and more work is needed to fully understand the nature of the M–CO bond in these compounds. A single-crystal X-ray analysis has been carried out on **2** in order to verify that the CO ligand is terminally bonded to Pd and to determine the geometry of the cluster core (vide infra).

$[(PPh_3)Pd(AuPPh_3)_6](NO_3)_2$ (3$(NO_3)_2$) was synthesized by the reaction of a CH_2Cl_2 solution containing $Pd(acetate)_2$ and PPh_3AuNO_3 with H_2 at ambient temperature. The product was isolated in 87% yield as an air- and moisture-stable brown solid. This preparation is a significant improvement over the one previously reported.[1] Since **3** was not thoroughly characterized previously, some discussion is needed. The ^{31}P NMR spectrum (20 °C, CD_2Cl_2) of **3** showed two resonances with a relative intensity of 1:6. The peak assigned to the PPh_3 ligand bound to the Pd atom (δ 59.8) appeared as a septet, and the upfield resonance (δ 47.5) assigned to the $Au(PPh_3)$ ligands appeared as a doublet. The ^{31}P NMR spectrum of **3** is indicative of fluxional

(33) Maitlis, P. M.; Espinet, P.; Russell, M. J. H. In *Comprehensive Organometallic Chemistry*; Wilkinson, G., Ed.; Pergamon Press: Oxford, England, 1982; Vol. 6, Chapters 38.2, 38.3, 38.4.

(34) Braunstein, P.; de Meric de Bellefon, C.; Ries, M.; Fischer, J.; Bouaoud, S.-E. *Inorg. Chem.* **1988**, *27*, 1327.

(35) Mann, B. E.; Taylor, B. F. *^{13}C NMR Data for Organometallic Compounds*; Academic Press: London, 1981; p 181.

behavior in solution. Positive ion FABMS analysis of $3(PF_6)_2$ gave a spectrum with well-resolved peaks. An analysis of the isotopic ion distribution pattern for the highest mass peak gave a most abundant mass ion of m/z 3267.2, which corresponds to the ion pair $[(PPh_3)Pd(AuPPh_3)_6(PF_6)]^+$. A complete analysis of the fragmentation pattern suggested that the neutral compound was $[(PPh_3)Pd(AuPPh_3)_6](PF_6)_2$. In agreement with this formulation, the conductance of **3** in CH_3CN showed it to be a 1:2 electrolyte, whether the counterion was NO_3^- or PF_6^-. Unfortunately, we have not been able to obtain X-ray-quality crystals of **3** so a determination of its structure has not been made. However, it is likely to have the same structure as its Pt analogue, $[(PPh_3)Pt(AuPPh_3)_6]^{2+}$.[18]

Compound **3** is a 16-electron compound and therefore is expected to undergo nucleophilic addition of 2-electron donor ligands such as CO or PR_3. Reaction with 1 atm of CO did not occur as monitored by IR spectroscopy although a stable CO adduct, $[(CO)(PPh_3)Pt(AuPPh_3)_6]^{2+}$, was readily formed with the Pt analogue.[18] Reaction did occur, however, with the phosphite ligand $P(OCH_2)_3CCH_3$, leading to the formation of the 18-electron compound $[(P(OCH_2)_3CCH_3)_2Pd(AuPPh_3)_6]^{2+}$ (**4**). Apparently the small cone angle of $P(OCH_2)_3CCH_3$ (101° compared with 145° for PPh_3)[36] favors the addition of two phosphite ligands with loss of the PPh_3 bound to Pd. The characterization data are consistent with this formulation. The ^{31}P NMR spectrum (20 °C, CD_2Cl_2) of **4** showed two resonances with a relative intensity of 1:3. The resonance assigned to the phosphite ligands (δ 185.1) appeared as a septet, and the upfield resonance (δ 44.3) assigned to the $AuPPh_3$ groups bonded to Pt appeared as a triplet. The ^{31}P NMR spectrum of **4** is indicative of fluxional behavior in solution. The ^1H NMR spectrum (20 °C, CD_2Cl_2) of **4** showed three resonances at δ 7.4–6.6, 3.43, and 0.40 ppm with a relative intensity of 15:2:1. The resonance assigned to the phenyl protons (δ 7.4–6.6) appeared as series of multiplets. The resonance (δ 3.43) assigned to the OCH_2 protons of the phosphite ligands appeared as a broad singlet. The most upfield resonance (δ 0.40) assigned to the CCH_3 protons of the methyl backbone in the phosphite ligands also appeared as a broad singlet. ^1H NMR spectroscopy showed no evidence for hydride ligands.

Positive ion FABMS analysis of $4(NO_3)_2$ gave a spectrum with well-resolved peaks. An analysis of the isotopic ion distribution pattern for the highest mass peak gave a most abundant mass ion of m/e 3219.4, which corresponded to the ion $[(P(OCH_2)_3CCH_3)_2Pd(AuPPh_3)_6(NO_3)]^+$. A complete analysis of the fragmentation pattern suggested that the neutral compound was $(P(OCH_2)_3CCH_3)_2Pd(AuPPh_3)_6(NO_3)_2$. In agreement with this formulation, the conductance of **4** in CH_3CN showed it to be a 1:2 electrolyte.

The addition of an excess of $P(OCH_3)_3$ to **1** gave the new 18-electron compound $[(P(OCH_3)_3)Pd(AuPPh_3)_6(AuP(OCH_3)_3)_2](NO_3)_2$ (**5**). The characterization data are consistent with the formulation of **5** as a derivative of **1** in which two PPh_3 ligands on the peripheral gold sites of the metal cluster core have been replaced with $P(OCH_3)_3$ ligands and a $P(OCH_3)_3$ ligand is also bonded directly to Pd. The ^{31}P NMR spectrum (20 °C, CD_2Cl_2) of **5** showed three broad resonances with a relative intensity of 1:2:6. At −90 °C the slow-exchange region was obtained and nine multiplet resonances were resolved corresponding to the nine different phosphorus atoms in the compound. The multiplets were complex, and coupling constants and assignments were not determined. This result indicates that the core geometry of **5** has all nine phosphorus atoms in nonequivalent environments. A single-crystal X-ray analysis has been carried out (vide infra) and supports this observation in the solid state. ^1H NMR spectroscopy showed no evidence for hydride ligands.

Positive ion FABMS analysis of $5(BF_4)_2$ gave a spectrum with well-resolved peaks. An analysis of the isotopic ion distribution pattern for the highest mass peak gave a most abundant mass ion of m/e 3801.9, which corresponded to the ion pair $[(P(OCH_3)_3)Pd(AuPPh_3)_6(AuP(OCH_3)_3)_2(BF_4)]^+$. A complete analysis of the fragmentation pattern suggested that the neutral compound was $(P(OCH_2)_3CCH_3)_2Pd(AuPPh_3)_6(BF_4)_2$. In agreement with this formulation, the conductance of **5** in CH_3CN showed it to be a 1:2 electrolyte.

Electrochemistry of 1. The electrochemistry of **1** was investigated by cyclic voltammetry (CV) and differential-pulse polarography (DPP) with use of CH_2Cl_2 and CH_3CN as solvents. The details of this study will be published elsewhere when data on more compounds are available, but it is important to establish the general electrochemical properties of **1** at this time, since they are relevant to other data presented in this paper. Compound **1** was electrochemically reduced by two stepwise, reversible one-electron transfers, thus showing an EE reduction mechanism (eq 1). The analysis of the data was done as previously described

$$Pd(AuPPh_3)_8^{2+} + e^- \rightleftharpoons Pd(AuPPh_3)_8^{+} + e^- \rightleftharpoons Pd(AuPPh_3)_8^{0} \quad (1)$$

for isoelectronic $[Pt(AuPPh_3)_8]^{2+}$ and $[Au(AuPPh_3)_8]^{3+}$ and the results are similar.[21] The results are summarized in Table V and are compared to those reported for the Pt- and Au-centered analogues.[21] The chemical reversibility of these reductions was established by cyclic voltammetry, as well-shaped reoxidation waves were seen in the backward scans with i_b/i_f ratios of 0.90 and 1.0 for scan rates of 100 and 200 mV/s, respectively, for CH_2Cl_2 solution. It is interesting to note the large shift to more negative reduction potentials in compound **1** compared to $Au(AuPPh_3)_8^{3+}$ (ca. 0.8 V) and $Pt(AuPPh_3)_8^{2+}$ (ca. 0.2 V). The difference of about 0.6 V between the Au- and Pt-centered clusters has been ascribed to a shift to a higher energy level of the LUMO in $Pt(AuPPh_3)_8^{2+}$ as compared with that for $Au(AuPPh_3)_8^{3+}$ and a concomitant increase of the electron density on the platinum atom.[21] This explanation was based on results of SCC-EHMO calculations.[21] The shift to even more negative potentials for the Pd-centered cluster **1** was unexpected, since this suggests that the Pd atom is more electron rich than its Pt analogue. Since the Pd- and Pt-centered clusters have nearly identical centered-crown structures in the solid state,[1,2] it was expected that the Pd compound would be easier to reduce than its Pt analogue. The observed result suggests that something is unusual with the Pd compound and further study is needed. Recall that **2**, the CO adduct of **1**, also showed unusual IR ν(CO) and ^{13}C NMR data (vide infra).

Crystal Structures of $[(CO)Pd(AuPPh_3)_8]^{2+}$ (2) and $[(P(OCH_3)_3)Pd(AuPPh_3)_6(AuP(OCH_3)_3)_2]^{2+}$ (5). These clusters are very similar in that both have the general formulation $[LPd(AuP)_8]^{2+}$. The solid-state structures of the cluster cores of **2** and **5** are nearly identical, as is evident from their ORTEP representations shown in Figures 1 and 2, respectively. A comparison of selected distances and angles within the metal cores (Table IV) confirms the close similarity of their geometries. The geometry of these 18-electron clusters is best described as a fragment of a centered icosahedron, as shown in Figure 3.

The structure of **2** consists of eight $Au(PPh_3)$ units bonded to a central Pd atom. There is a CO ligand bound in a unidentate fashion to Pd, giving the central Pd atom a coordination number of 9. The metal framework in **2** is very similar to that found in the isoelectronic Pt analogue $(CO)Pt(AuPPh_3)_8^{2+}$.[2]

There is a major geometric difference in the structure of compounds **1** and **2**. The 16-electron cluster **1** has a toroidal geometry best described as that of a centered crown.[1] Upon addition of CO to form the 18-electron cluster **2**, the geometry changes into the more spherically shaped icosahedral fragment shown in Figures 1 and 3. The increased coordination number of Pd results in a weakening of the metal–metal interactions, as reflected in the increased bond lengths in the metal core. Thus, the average Pd–Au distance increased from 2.618 Å (range 2.611–2.624 Å)[1] in **1** to 2.673 Å (range 2.626–2.727 Å) in **2** and the average Au–Au distance increased from 2.792 Å (range 2.765–2.804 Å)[1] in **1** to 2.912 Å (range 2.804–3.091 Å) in **2**. The average Pd–Au bond distance in **2** is very similar to the average Pt–Au distance in $(CO)Pt(AuPPh_3)_8^{2+}$ (2.675 Å, range 2.651–2.703 Å).[2] The average Au–Au bond distance in **2** is slightly shorter than that found

(36) Tolman, C. A. *Chem. Rev.* **1977**, *77*, 313.

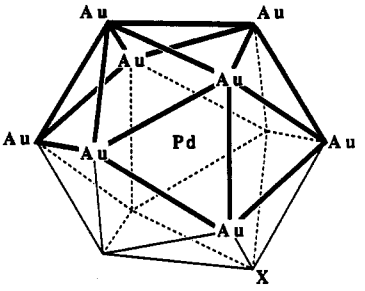

$[(CO)Pd(AuPPh_3)_8]^{+2}$ (2)

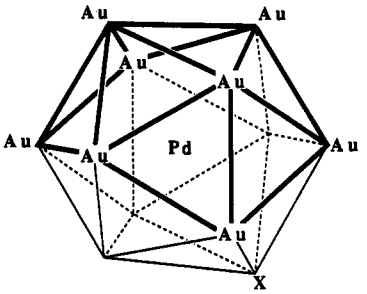

$[(P(OCH_3)_3)Pd(AuPPh_3)_6(Au(P(OCH_3)_3)_2]^{+2}$ (5)

Figure 3. Metal-core geometries of the 18-electron clusters **2** and **5** shown as fragments of the centered icosahedron. The darkened lines represent bonding interactions between metal atoms. The central Pd atom is bonded to all of the peripheral metals, but these bonds are not shown for the sake of clarity. The vertex labeled X is the direction to which the CO or $P(OCH_3)_3$ ligand bound to Pd lies.

in $(CO)Pt(AuPPh_3)_8^{2+}$ (2.987 Å, range 2.83–3.15 Å).[2] The Au–P distances in **2** (average 2.29 Å, range 2.27–2.33 Å) are slightly longer than those found in **1**[1] (average 2.275 Å, range 2.261–2.294 Å). The Au–PPh_3 vectors are approximately trans to the transition-metal atom (average Pd–Au–P = 164.8°), which is a general trend found in complexes of this type.[3,14,18] The Pd–C bond distance (1.90 Å) and the C–O bond length (1.07 Å) in **2** is in the normal range for metal carbonyls.[2,18,34]

The $LPdAu_8$ metal core geometry of **5** is similar to that of **2**. The central Pd atom with a coordination number of 9 has six $Au(PPh_3)$ units, two $Au(P(OCH_3)_3$ units, and one $P(OCH_3)_3$ ligand bonded to it. It is interesting that the coordination of the larger $P(OCH_3)_3$ ligand to the Pd atom in **5** results in a geometry that is nearly identical with that of the CO adduct **2**. Compound **5** is the first example of a transition-metal–gold cluster compound where some of the peripheral gold atoms have been substituted by phosphite ligands. The reason for the substitution of only two of the PPh_3 ligands is not understood but as with monosubstituted isonitrile derivatives of $[Pt(AuPPh_3)_8]^{2+}$ is thought to be primarily the result of steric factors.[2]

The average Pd–Au bond distance in **5** (2.709 Å, range 2.682–2.747 Å) is longer than that in **1** (average 2.618 Å, range 2.611–2.624 Å) and in **2** (average 2.673 Å, range 2.626–2.727 Å). The average Au–Au bond distance in **5** (2.901 Å, range 2.817–3.014 Å) is slightly shorter than in **2** (average 2.912 Å, range 2.804–3.091 Å) but longer than found in **1** (average 2.792 Å, range 2.765–2.804 Å).[1]

The Pd–P bond distance (2.29 Å) and average Au–P distances in **5** (Au–PPh_3 = 2.31 Å and Au–$P(OCH_3)_3$ = 2.26 Å) are within the normal range found in other transition-metal–gold cluster compounds.[1-3,18] The average Pd–Au–P angle in **5** (168.6°) is more trans than in **1** (160.4°) or **2** (164.8°) but is very similar to that found in $(CO)Pt(AuPPh_3)_8^{2+}$ (168.1°).[2] The largest difference in the geometry between **2** and **5** occurs with some of these Pd–Au–P angles. In **2**, the Pd–Au–P angles, which involve the four phosphorus atoms adjacent to the CO ligand, show the largest deviation from linearity (average for P1, P1A, P4, and P4A is 156.8°). The other four Pd–Au–P angles in **2** average 172.8°. This difference is not as pronounced in **5**, where the average angles for the same two sets are 166.5 and 170.6°, respectively. Since the bending of the phosphine ligands is in the direction of the CO ligand, this difference is due to the smaller steric size of CO ligand compared to the phosphite. A similar but less pronounced bending has also been observed with $[(CO)Pt(AuPPh_3)_8]^{2+}$.[2]

Acknowledgment. This work was supported by the National Science Foundation (Grant CHE-8818187) and by the University of Minnesota. We also thank the Fundação De Amparo À Pesquisa Do Estado De São Paulo for support of Dr. Felicissimo's visit to Minnesota. Acknowledgment is also made to Professor J. J. Steggerda and his co-workers who kindly carried out the electrochemical analysis.

Supplementary Material Available: Figures S1 and S2, displaying the PLUTO drawings of **2** and **5**, Table SI, listing the complete crystal data and data collection parameters, and Tables SII–SIX, listing general temperature factor expressions, final positional and thermal parameters for all atoms including solvate molecules, and distances and angles (39 pages); Tables SX and SXI, listing observed and calculated structure factor amplitudes (96 pages). Ordering information is given on any current masthead page.